NeuroImage 326 (2026) 121691

Contents lists available at ScienceDirect

NeuroImage

journal homepage: www.elsevier.com/locate/ynimg

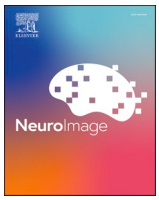

Intolerance of uncertainty modulates amygdala habituation to emotional faces

Jihye Jeon [a], Hakin Kim [b], Juyoen Hur [b], M. Justin Kim [a,c,d,*]

[a] Department of Psychology, Sungkyunkwan University, Seoul, 03063, South Korea
[b] Department of Psychology, Yonsei University, Seoul, 03722, South Korea
[c] Department of Brain Science and Engineering, Sungkyunkwan University, Suwon, 16419, South Korea
[d] Center for Neuroscience Imaging Research, Institute for Basic Science, Suwon, 16419, South Korea

ARTICLE INFO

Keywords:
Amygdala
Habituation
Intolerance of uncertainty
Emotion
fMRI

ABSTRACT

People differ widely in how they perceive uncertain *situ*ations as stressful and threatening. Intolerance of uncertainty (IU) captures these individual differences while operating as a transdiagnostic and transsituational risk factor. In the present study, we investigated how individual differences in the sensitivity to uncertainty, rather than broader anxious traits, influence the temporal dynamics of amygdala habituation to emotional faces. Eighty-five human participants (18 males) completed an emotional face-matching task during functional magnetic resonance imaging (fMRI) scanning. The habituation slope – reflecting the rate at which amygdala activation decreased across repeated face blocks – covaried with individual IU levels. Participants with lower IU showed steeper habituation slopes, indicating a rapid decrease in amygdala responses, whereas those with higher IU exhibited attenuated slopes, reflecting sustained activation over time. This effect remained significant after controlling for general trait anxiety. Because emotional faces convey varying degrees of affective and social ambiguity, they are potent elicitors of vigilance in individuals' sensitivity to uncertainty. This observed relationship between IU and amygdala habituation suggests that reduced neural adaptation to emotional stimuli may represent a core mechanism linking uncertainty sensitivity to anxiety vulnerability.

1. Introduction

Navigating uncertainty is a fundamental part of human experience, yet people vary widely in their tolerance for ambiguous and unpredictable situations. Intolerance of uncertainty (IU) reflects individual differences in the difficulty of tolerating uncertain future outcomes and is now understood as a transdiagnostic and transsituational risk factor (Dugas et al., 2001; Dugas et al., 2025). Cognitive theories conceptualize IU as biased information processing, in which uncertainty is appraised as threatening through a selective focus on potential danger (Beck et al., 1985). Individuals with high IU experience negative emotional responses when faced with a lack of salient or sufficient information (Carleton, 2016). They also show differences in cognitive, behavioral, and emotional functioning under uncertainty, particularly in heightened attentional engagement and anticipatory responding to uncertain stimuli (Buhr and Dugas, 2002; Tanovic et al., 2018; Morriss et al., 2023). Importantly, uncertainty is particularly salient in social contexts, where outcomes depend on others and are therefore inherently difficult to predict (FeldmanHall and Shenhav, 2019). This variability likely underlies the strong link between IU and internalizing symptoms across clinical and nonclinical populations (Dugas et al., 2001).

Neuroimaging studies of IU highlight the amygdala, a key region in uncertainty processing (Grupe and Nitschke, 2013; Greifenberger et al., 2025). This region plays a core role in detecting and directing attention toward motivationally salient stimuli, particularly those that are uncertain or ambiguous (Davis and Whalen, 2001). This function has been consistently supported by findings from both animal and human studies (Rosen and Schulkin, 1998; Whalen, 1998; Whalen et al., 2001; Rosen and Donley, 2006; Herry et al., 2007), showing heightened amygdala responses to temporally unpredictable events (e.g., unpredictably timed sound pulses) and to ambiguous emotional cues such as surprised faces that require contextual interpretation (Kim et al., 2004; Davis et al., 2016; Kim et al., 2017).

A prominent characteristic of the amygdala is its tendency to rapidly habituate to repeated stimuli. Habituation, defined as a decrease in neural response to repeated stimuli (Thompson and Spencer, 1966),

* Corresponding author.
E-mail address: minuekim@skku.edu (M.J. Kim).

https://doi.org/10.1016/j.neuroimage.2026.121691
Received 21 November 2025; Received in revised form 29 December 2025; Accepted 3 January 2026
Available online 4 January 2026

allows the organism to disengage from inputs that no longer signal threat or novel information (Rankin et al., 2009). As stimuli that were once uncertain become predictable through repetition, the amygdala habituates by showing a reduced response (Bordi and LeDoux, 1992; Herry et al., 2007). The rate of this attenuation varies substantially across individuals, reflecting differences in psychological resilience and adaptive emotion regulation (Davidson, 2002; Schuyler et al., 2014). Amygdala habituation to emotional faces has been consistently observed (Breiter et al., 1996; Phillips et al., 2001; Fischer et al., 2003) and reduced habituation has been associated with clinical groups with altered socioemotional processing (Shin et al., 2005; Kleinhans et al., 2009; Kim et al., 2019). It also serves as a reliable within-subject neural measure in emotional face tasks (Plichta et al., 2014; Gee et al., 2015).

Research directly linking amygdala habituation to IU in emotional face paradigms remains limited. Previous studies have largely focused on paradigms involving conditioned threat or aversive stimuli to evoke uncertainty-related responses (Schienle et al., 2010; Morriss et al., 2016a; 2016b). Investigating whether IU is also associated with altered amygdala habituation to facial expressions may offer insights into more generalizable neural processes that extend beyond threat-based paradigms. In this study, we aimed to characterize amygdala habituation by estimating the linear slope of fMRI signal change over time. This method offers greater sensitivity to the temporal dynamics of neural response than approaches that simply compare activation between the first and last stimulus blocks (Lane et al., 2013; Plichta et al., 2014; McDiarmid et al., 2017). Before testing our primary hypothesis, we first sought to replicate the well-established finding that amygdala activation decreases across repeated presentations of emotional faces, reflecting a negative habituation slope. We further hypothesized that IU would moderate this effect, such that higher IU would be associated with greater attenuation of habituation rate as observed in fear extinction and neuropsychiatric studies (Morriss et al., 2015; 2016b; McDiarmid et al., 2017), whereas lower IU would predict stronger decreases in amygdala activation over time. To test the specificity of this effect, we expected the moderating role of IU to remain significant after controlling for general trait anxiety (Morriss et al., 2021). In addition, we examined the anterior insula as a theoretically relevant comparison region, given its established role in intolerance of uncertainty (Simmons et al., 2008; Gorka et al., 2016).

2. Materials and methods

2.1. Participants

Participants in the present study were drawn from a larger longitudinal project focused on elucidating the etiological processes that confer risk for the development of mood and anxiety disorders (see Supplementary Materials for details). Of the 111 participants who completed the MRI scanning sessions, 26 were excluded from analyses due to technical issues ($n = 3$), non-compliance ($n = 11$), excessive head motion ($n = 10$), or low temporal signal-to-noise ratio (tSNR; see details below; $n = 2$). Participants were excluded for motion if their mean framewise displacement (FD) exceeded 0.25 mm. The resulting final sample included 85 participants (18 males; mean age = 22.5 years). All participants were Korean young adults under the age of 26 residing in the Seoul metropolitan area. Only those without current internalizing disorders (e.g., major depressive disorder, generalized anxiety disorder, panic disorder, social anxiety disorder) and no history of neurological or alcohol/substance-related problems were included. Participants also reported no history of psychiatric treatment, psychiatric medication use, or suicidal ideation. All procedures were approved by the Institutional Review Board (IRB) of Yonsei University, Seoul, South Korea and written informed consent was obtained from all participants.

2.2. Questionnaires

2.2.1. Intolerance of uncertainty scale

The Intolerance of Uncertainty Scale-12 (IUS-12) is a short form of the original 27-item Intolerance of Uncertainty Scale (Freeston et al., 1994). Seven items assess the prospective IU – desire for predictability – while five items assess the inhibitory IU, reflecting uncertainty paralysis. All items are rated on a 5-point Likert scale ranging from 1 (“not at all characteristic of me”) to 5 (“entirely characteristic of me”).

2.2.2. State-trait anxiety inventory

The State-Trait Anxiety Inventory Questionnaire (STAI; Spielberger, 1983) is a validated 40-item self-report questionnaire comprising two 20-item subscales that separately assess state and trait anxiety. Only the trait subscale (STAI-T), which measures participants’ general tendency to feel anxious, was included in the analysis. Items are rated on a 4-point Likert scale ranging from 1 (“almost never”) to 4 (“almost always”).

2.3. Emotional face-matching task

Amygdala activity was assessed using a modified version of the emotional face-matching task designed to engage the emotional processing system, similar to prior work (Kim et al., 2022; Fig. 1). The task comprised four emotional categories (fearful, happy, surprised, and neutral), each presented twice, yielding a total of eight emotional face blocks. These were interleaved with eight shape blocks, which served as the control condition. The order of emotional face categories was counterbalanced across participants using 12 pseudo-randomized sequences based on a Latin Square design to minimize potential ordering effects (Table S1). During each emotional face block, three faces from the same emotional category were presented in a triangular configuration: the top face served as the target, and participants were instructed to select the matching face from the two faces at the bottom. Each trial lasted 3 s, followed by a 1-s interstimulus interval. Each block consisted of six trials, resulting in a total duration of 24 s. Every four task blocks were followed by a 15-s fixation period and the overall task duration was 435 s. Reaction time and response accuracy were obtained for each trial. Face stimuli were taken from the Racially Diverse Affective Expression (RADIATE) face stimulus set (Conley et al., 2018) and were balanced for race and gender across trials; a total of 48 stimulus images (16 identities) were used.

2.4. fMRI data acquisition

MRI scans were acquired at the Siemens Healthineers Research MRI Center located at Yonsei University, using a Siemens MAGNETOM VIDA 3T scanner with a 32-channel head coil. Structural images were acquired using a T1-weighted MPRAGE (magnetization-prepared rapid acquisition gradient echo) sequence with the following parameters: TR = 2.300 ms, TE = 2.26 ms, flip angle = 8°, field of view = 256 mm, matrix size = 256 × 256, and voxel resolution of 1 mm^3. Functional data were collected using a multiband echo-planar imaging (EPI) sequence optimized for high spatial and temporal resolution (acceleration factor = 3; TR = 1.500 ms; TE = 30 ms; flip angle = 80°; FOV = 220 mm; matrix = 110 × 110; 69 axial slices; voxel size = 2 mm^3). A set of 10 EPI images with reverse phase encoding direction was acquired to correct susceptibility-related distortions.

2.5. fMRI data preprocessing

fMRI data were preprocessed using fMRIPrep 21.0.2 (Esteban et al., 2019). Preprocessing included generation of a blood-oxygen-level-dependent (BOLD) reference image, motion correction, susceptibility distortion correction, slice-timing correction, and co-registration of functional images to the corresponding T1-weighted image. Preprocessed BOLD images were spatially normalized to

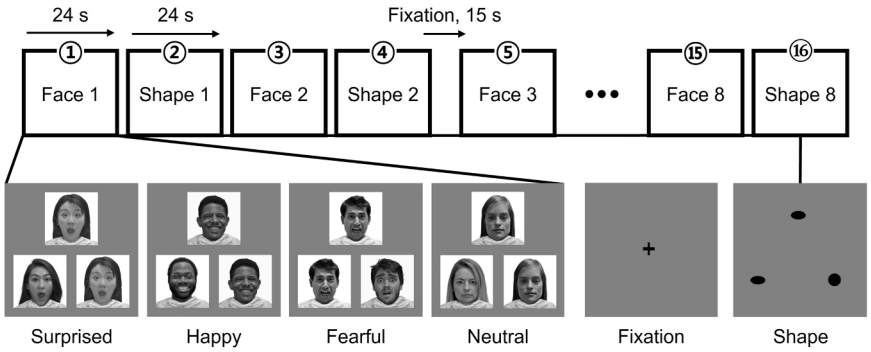

Fig. 1. Schematic of the emotional face-matching task. each block lasted 24 s and consisted of six trials. emotional face blocks (surprised, happy, fearful, neutral) were alternated with shape-matching blocks, with every four task blocks followed by a 15 s fixation period. The order of emotional conditions was counterbalanced across participants.

MNI152NLin2009cAsym standard space and spatially smoothed with a 6 mm full-width at half-maximum Gaussian kernel using 3dmerge in AFNI (Cox, 1996; Cox and Hyde, 1997). Confound regression was performed using six rigid-body motion parameters (three translations and three rotations). Finally, high-pass filtering was applied with a 128 s cut-off. As part of quality assurance, mean EPI image was overlaid on the T1-weighted anatomical image averaged across all subjects to assess spatial normalization and bilateral amygdala coverage (Fig. S1).

2.6. Amygdala signal quality assessment

Temporal signal-to-noise ratio (tSNR) was calculated for the left and right amygdala, as the amygdala BOLD signal is particularly susceptible to artifacts caused by inhomogeneous magnetic fields in the ventral brain regions, as well as signal dropout due to its proximity to the air-filled sinuses. For each participant, the mean signal across the entire time series was computed on a voxel-by-voxel basis, which was subsequently divided by the standard deviation. Mean tSNR of the bilateral amygdala was 122.4 ($SD = 18$). Participants with tSNR values exceeding 2 *SD*s below the mean were excluded from the analysis ($n = 2$).

2.7. fMRI data analysis

fMRI data were analyzed within the SPM12 (https://www.fil.ion.ucl.ac.uk/spm) to generate region of interest (ROI) masks and block-wise beta estimates. Bilateral amygdala was selected as the ROI for subsequent habituation analyses, given its central role in emotional face processing and its well-documented tendency to exhibit habituation across repeated stimulus presentations. To generate a group-level amygdala mask, the emotional faces > shapes contrast was first estimated for each participant using a first-level general linear model (GLM) (Mende-Siedlecki et al., 2013). These contrast images were then entered into a second-level GLM to identify voxels within the amygdala that show a significant response to emotional faces compared to shapes. The Harvard–Oxford subcortical atlas (right and left amygdala) was applied to the second-level contrast map (faces > shapes). Voxels within the atlas-defined amygdala that showed significant activation ($p < .05$, FWE-corrected within mask) were identified and extracted as the bilateral amygdala ROI for subsequent analyses. As a control analysis, bilateral anterior insula regions of interest were defined using the labels *Neuromorphometrics* implemented in SPM (Fig. S2).

Subsequently, first-level GLMs were specified again for each participant to estimate beta values reflecting amygdala responses across repeated emotional face blocks. The shape condition was modeled as a control regressor collapsing across all shape blocks to reduce the number of predictors and to ensure stable estimation of effect sizes by avoiding unnecessary model complexity (Silverman et al., 2019). Two complementary modeling approaches were implemented. First, we estimated separate block-wise beta coefficients for each of the eight face blocks (b_{face}):

$$y(t) = \sum_{i=1}^{8} b_i^{\text{face}} x_i^{\text{face}}(t) + b_{\text{shape}} x_{\text{shape}}(t) + \text{nuisance}(t) + \varepsilon(t)$$

This block-wise modeling approach was also applied to the bilateral anterior insula as a control analysis.

Second, we modeled a linear parametric modulation estimate (b_{PM}) for single face regressor:

$$y(t) = b_{\text{face}} x_{\text{face}}^{(t)} + b_{\text{PM}} \left[x_{\text{face}}^{(t)} \cdot p(t) \right] + b_{\text{shape}} x_{\text{shape}}(t) + \text{nuisance}(t) + \varepsilon(t)$$

where $p(t)$ represents a linear parametric modulator coding the repetition order (1-8). These estimates served as input for subsequent group- and individual level habituation analyses described below.

2.8. Habituation analyses

We estimated habituation slope at both the group and individual levels to examine whether IU influences the rate of amygdala habituation over time. This two-level approach was adopted to enhance robustness and minimize potential estimation bias across analytic strategies. We designated the group-level model as the primary analytic approach, with the pseudo-randomized block order ensuring balanced representation of the four emotion categories across participants. At the group level, we first estimated a single habituation slope by averaging block-wise responses across participants and tested whether IU scores moderated this group-level slope. At the individual level, we estimated a separate habituation slope for each participant and examined whether IU scores predicted the variability of these slopes. In both analyses, IU and STAI-T were treated as continuous individual-difference variables.

Because each emotion category was presented only twice and emotion presentation order was pseudo-randomized across participants, emotion-specific habituation effects could not be reliably estimated. Accordingly, we focused on habituation across repeated face blocks in general. As a *post-hoc* analysis, we tested whether habituation slopes were modulated by emotion presentation order. In the absence of consistent sequence-related effects, emotion presentation order was not incorporated into the primary analyses. Results of these *post-hoc* analyses are reported in Supplementary Materials (Table S2).

2.9. Group-level habituation analysis

Following previous work that employed block-wise beta estimates to quantify habituation (Plichta et al., 2014), we used the beta estimates obtained from the first-level GLM (b_{face}). Mean b_{face} values were plotted to visualize the overall pattern of amygdala activation and to examine whether the pattern differed as a function of IU level. Within-subject

95% confidence intervals (CIs) were computed using the normalization method proposed by Cousineau (2005) with Morey's (2008) correction. We additionally tested whether CI width reflected differences in within-subject variability across subgroups using Welch's test.

To statistically test habituation effects and their moderation by individual differences, we conducted a series of nested model comparisons by sequentially adding predictors in a linear mixed-effects modeling (LMM) framework. LMMs were performed in R (version 4.4.2) using the lme4 and emmeans packages (Bates et al., 2015; Lenth, 2023). The eight block-wise beta values for the face condition were treated as repeated measures within subjects, and block order (1-8) was modeled as a continuous measure of time. We sequentially specified a set of LMMs that (i) tested habituation with Time, (ii) added IU and Time x IU to assess the moderation effect, and (iii) added STAI-T and Time x STAI-T. Sex was included as a covariate. All continuous predictors (Time, IU, STAI-T) were mean-centered. Random intercepts and slopes for Time were initially modeled for each subject, with a diagonal covariance structure specified for the repeated measure, to account for between-subject differences in baseline activation as well as unexplained variance in slopes. However, the random slope was excluded from the final models due to convergence issues. Models were estimated using restricted maximum likelihood (REML). The final model equation was as follows:

$$b_{face} \sim \text{Sex} + \text{Time} + \text{IU} + \text{STAI-T} + \text{Time} * \text{IU} + \text{Time} * \text{STAI-T} + (1|\text{subject}).$$

The same model was applied to beta estimates from the anterior insula for the control analysis. Significant interactions were followed up with simple slopes analyses using *emtrends* function in the *emmeans* package. Simple slopes for Time were estimated and tested for significance at low (-1 *SD*), mean (0 *SD*), and high (+1 *SD*) levels of IU, with *p*-values based on the Kenward-Roger method.

2.9.1. Individual-level habituation analysis

We conducted an individual-level analysis to obtain person-specific slope estimates and to confirm the findings derived from the group-level analyses. Habituation slopes were estimated at the individual level within the standard SPM GLM framework. For each participant, the eight emotional face blocks were modeled as a single regressor, with block order (1-8) specified as a parametric modulator to capture linear signal changes across blocks. This approach yielded a parametric modulation coefficient (b_{PM}), referred to as habituation slope, for each participant. More negative values indicating steeper decreases in amygdala response and less negative reflecting sustained responses. The resulting habituation slopes were then entered into linear regression analyses, including IU as predictors and STAI-T and sex as covariates. Regression analyses were implemented in R using the lm function.

3. Results

3.1. Self-reported and behavioral data

Descriptive statistics and internal reliability estimates for self-reported measures, including IU and STAI-T, are summarized in Table 1. As expected, IU had a significant positive correlation with STAI-T ($r = .53, p < .001$). Descriptive statistics for accuracy and reaction time across conditions are presented in Table 2.

Table 1
Sample characteristics and descriptive statistics.

Measure	Value
Sample size (N)	85
Sex (female/male)	67 / 18
Age (years)	22.5 (1.8), range 19-26
IU	2.48 (0.85), range 1.17-5.00, $\alpha = .90$
STAI-T	2.17 (0.48), range 1.40-3.45, $\alpha = .89$

Note. Values are mean (SD). Participants were non-clinical Korean young adults, residing in Seoul metropolitan area. Psychiatric status was assessed using self-report screening procedures as part of a larger longitudinal study.

3.2. Group-level habituation analysis

The faces > shapes contrast revealed significant bilateral amygdala activation (Fig. 2; Table 3). These clusters were used as bilateral amygdala ROI masks for the following habituation analyses. Block-wise trajectories of the estimated BOLD responses are shown in Fig. 2. In the overall sample, amygdala activation fluctuated across blocks with a modest downward tendency. Fluctuations were more pronounced in the high-IU group, whereas the low-IU group showed a more consistent decrease. The wider confidence intervals observed in the IU subgroup panels are likely attributable to differences in sample size, because the high-IU group ($M = 0.52, SD = 0.18, n = 14$) and the low-IU group ($M = 0.57, SD = 0.24, n = 17$) did not significantly differ in within-subject variability ($t(28.75) = -0.63, p = .535$, Hedges' $g = -0.21$, 95% CI [−0.20, 0.11]). Individual subject trajectories are provided in the Supplementary Materials (Fig. S3) to illustrate inter-individual variability in block-wise responses underlying these descriptive patterns. For reference, the mean activation trajectory of the average IU group is also shown (Fig. S4).

We first fitted a LMM with Time as a fixed effect and sex as a covariate to test for habituation in amygdala responses across repeated face blocks. The effect of Time was not statistically significant ($b = -0.01, SE = 0.01, t(594) = -1.37, p = .172$), whereas sex showed a significant main effect, with females showing higher overall amygdala response than males ($b = 0.30, SE = 0.10, t(82) = 2.88, p = .005$). Although the main effect of Time was not significant, we next examined whether IU moderated the habituation effect, by adding IU and the Time x IU interaction to the model. The main effect of Time ($b = -0.01, SE = 0.01, t(593) = -1.37, p = .170$) and IU ($b = 0.06, SE = 0.05, t(82) = 1.18, p = .241$) were not significant. However, the Time x IU interaction was significant ($b = 0.03, SE = 0.01, t(593) = 2.53, p = .012$), indicating that the effect of Time on amygdala responses differed as a function of IU. Finally, to test the specificity of this effect, we included STAI-T and its interaction with Time in the model. Full results of the final model are presented in Table 4. After controlling for STAI-T, the Time x IU interaction remained significant, whereas the Time x STAI-T interaction was not, suggesting that the moderating effect was specific to IU. This effect was comparable in the left and right amygdala (Table S3, S4). In the anterior insula, neither the main effect of IU nor the Time x IU interaction reached statistical significance. Full results of the anterior insula control analysis are reported in the Supplementary Materials (Table S5).

Simple slopes analysis revealed that the effect of Time on amygdala activation differed across levels of IU (Fig. 3). At low levels of IU, greater decreases in amygdala response over time were observed ($b = -0.04, SE = 0.01, t(592) = -2.82, p = .005$), consistent with a typical habituation pattern. In contrast, mean levels of IU ($b = -0.01, SE = 0.01, t(592) = -1.37, p = .170$) and individuals with high IU ($b = 0.01, SE = 0.01, t(592) = 1.00, p = .317$) did not show significant changes in amygdala response over time, indicating relatively stable activation patterns.

Table 2
Averaged response times (ms) and accuracy rates (%) across participants for each stimulus category.

	Emotional Faces				Shapes
	Fear	Happy	Surprise	Neutral	
Response Time (ms)	830 (141)	869 (175)	874 (167)	818 (144)	773 (145)
Accuracy (%)	99 (8)	98 (11)	98 (14)	99 (9)	97 (16)

Note. Values are *M* (*SD*).

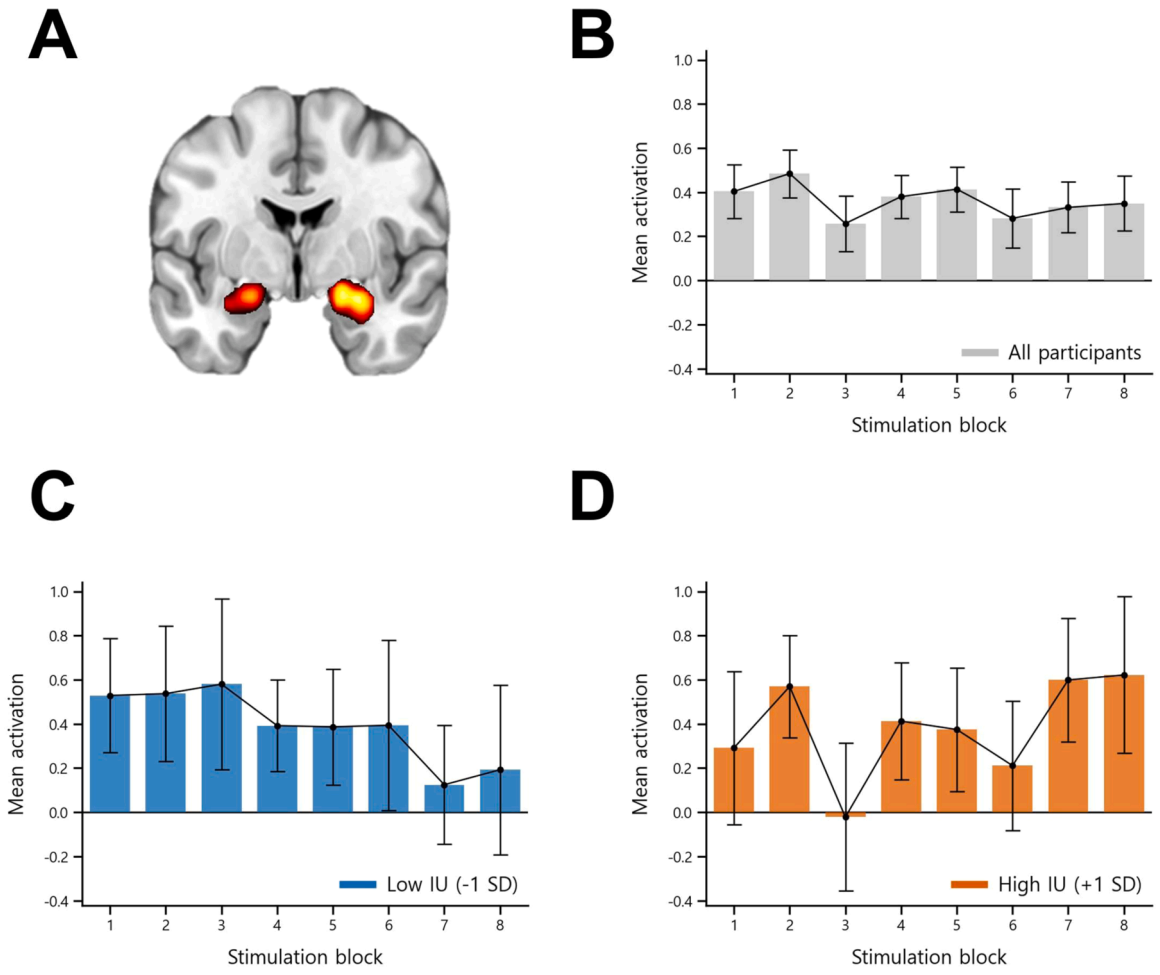

Fig. 2. Block-wise trajectories of amygdala activation across eight face blocks. (A) Group-level bilateral amygdala activation for the faces > shapes contrast ($p < .05$; FWE-corrected). (B) Average activation pattern across all participants. The *x*-axis represents block order (1–8), and the *y*-axis represents amygdala mean activation (b_{face}). Participants' IU scores were standardized (*z*-scored), and illustrative subgroups were defined using ±1 SD cut-offs to visualize potential differences in temporal patterns. (C) Participants with low IU (less than –1 *SD;* n= 17). (D) participants with high IU (greater than +1 *SD;* n=14). Stratification by IU level was conducted solely for visualization purposes to illustrate the general pattern of activation; IU was treated as a continuous variable in all statistical analyses. Bars and error caps depict mean parameter estimates and within-subject 95% CIs. The wider CIs observed in the subgroup panels primarily reflect reduced sample sizes relative to full sample, as Welch's test indicated no significant differences in within-subject variability between the high and low groups.

Table 3
Peak voxel coordinates and statistics for significant activations within the atlas-defined amygdala mask for the faces > shapes contrast ($p < .05$, FWE-corrected within mask). Coordinates are reported in MNI space.

			Coordinates at peak voxel				
cluster		*k*	*x*	*y*	*z*	*t*	$p_{FWE\text{-}corr}$
1	Right	516	20	-4	-14	14.63	< .001
	Right		28	-2	-18	13.52	< .001
2	Left	308	-18	-6	-14	12.25	< .001

3.3. Individual-level habituation analysis

To further support the group-level findings, we examined individual differences in habituation slopes using linear regression analyses. IU ($b = 0.03$, $SE = 0.01$, $t(81) = 2.12$, $p = .037$) significantly predicted individual habituation slopes, such that individuals with higher IU showed less negative habituation slopes (Fig. 4). In contrast, STAI-T ($b = -0.01$, $SE = 0.02$, $t(81) = -0.52$, $p = .604$) and sex ($b = -0.01$, $SE = 0.03$, $t(81) = -0.21$, $p = .835$) were not significant predictors, suggesting that individual differences in habituation were specifically associated with IU rather than STAI-T. Sex did not predict the rate of change over time.

Table 4
Linear mixed-effects model testing the effects of Time, IU, and STAI-T on amygdala activation.

Fixed effect					
	Estimate	*SE*	df	*t* statistic	*p value*
(Intercept)	0.08	0.10	81.00	0.80	0.426
Time	-0.01	0.01	592.00	-1.37	0.170
Sex (female)	0.35***	0.11	81.00	3.09	0.003
STAI-T	0.08	0.10	81.00	0.75	0.456
Time x STAI-T	-0.02	0.02	592.00	-0.68	0.496
IU	0.04	0.06	81.00	0.73	0.467
Time x IU	0.03*	0.01	592.00	2.56	0.011
Random effect					
	Variance	*SD*			
Subject (intercept)	0.11	0.34			
Residual	0.29	0.54			
Model fit					
	Marginal	Conditional			
R^2	0.05	0.32			

* $p < .05$
** $p < .01$
*** $p < .005$.

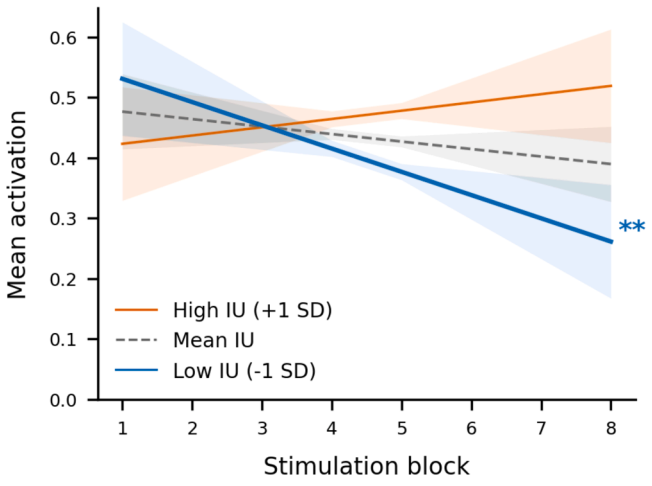

Fig. 3. Interaction between Time and IU on amygdala activation. lines represent estimated linear trends of amygdala activation across stimulation blocks at low (-1 *SD*), mean (0 *SD*), and high (+1 *SD*) levels of IU. Colored bands indicate 95% confidence intervals. The slope for low IU was significant ($p < 0.005$), whereas slopes for mean and high IU were not significant.

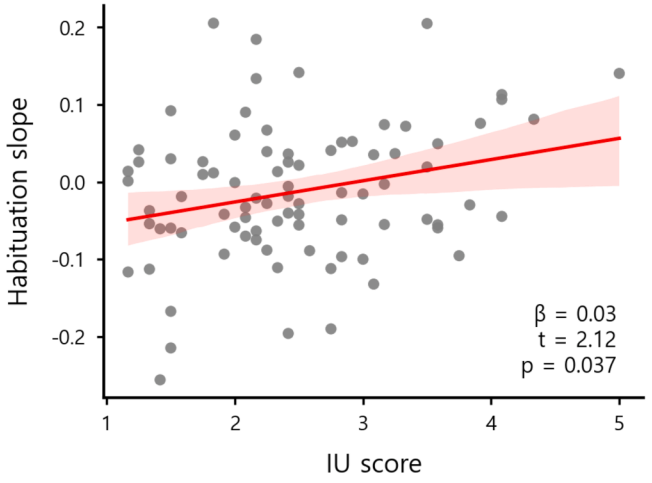

Fig. 4. Relationship between IU and individual amygdala habituation slopes, controlling for STAI-T and sex. Each point represents a participant's slope, and the red line indicates the fitted regression line with shaded 95% confidence interval. higher IU scores were associated with less negative habituation slopes, suggesting reduced amygdala habituation.

4. Discussion

Here we show that individual differences in intolerance of uncertainty – reflecting sensitivity to the unknown – modulate the rate of amygdala habituation probed with a widely used fMRI task that involves repeated presentation of emotional faces. Our analyses revealed that IU significantly moderated the amygdala habituation slope, such that individuals higher in IU showed greater attenuation of habituation rate, whereas those lower in IU demonstrated steeper decreases. This moderation effect remained significant even after controlling for general trait anxiety, which itself did not significantly influence the habituation slope of the amygdala. Moreover, this association was consistent when slopes were estimated separately for each participant, indicating convergent evidence across different modeling approaches to amygdala habituation. No corresponding IU-related effects were observed in the anterior insula, suggesting a degree of regional specificity.

Group-level analyses revealed a weak negative trend in amygdala activation across time, which was not statistically significant. Prior studies with healthy participants have typically reported significant decreases in amygdala activation to repeated face stimuli (Somerville et al., 2004; Plichta et al., 2014; Geissberger et al., 2020). However, many previous studies examined healthy individuals mainly as control groups in patient-control designs (Swartz et al., 2013; Williams et al., 2013), yielding relatively small samples of healthy participants. Methodological differences may also explain discrepancies, as prior studies used fewer blocks or collapsed responses into early versus late phases (Hariri et al., 2002; Somerville et al., 2004; Plichta et al., 2014), whereas the present study included eight blocks. Beyond such methodological factors, individual differences may also contribute to variability in habituation. Consistent with prior evidence of inter-individual variability in amygdala habituation within healthy samples (Geissberger et al., 2020), the observed variability may reflect underlying idiosyncratic characteristics, including IU. Additionally, it is worth noting that males exhibited higher amygdala activation than females. Although some studies have reported sex differences in amygdala responsivity depending on the valence of emotional stimuli (Stevens and Hamann 2012), the present finding should be interpreted with caution given the small number of male participants ($n = 18$) relative to females ($n = 67$).

A central aim of this study was to determine whether IU accounts for individual differences in the temporal dynamics of amygdala responsivity to emotional faces. With this in mind, we found that individuals with lower IU exhibited more rapid amygdala habituation to repeated emotional faces, whereas higher IU was associated with a more sustained response. Although prior work explicitly examining individual differences in IU and amygdala habituation within an emotional face paradigm has been relatively limited, related evidence offers a useful context for interpreting the present findings. Studies using fear conditioning paradigms have shown that higher IU is linked to sustained amygdala responsivity and difficulty downregulating threat responses during extinction learning (Dunsmoor et al., 2015; Morriss et al., 2015). These findings support the idea that IU-related differences emerge under conditions where explicit threat is absent, reflecting the psychological construct's core characteristics.

It is important to consider why emotional face stimuli may inherently convey uncertainty, and how such uncertainty could be differently processed at the neural level depending on the different degrees of IU. Emotional facial expressions convey complex and often ambiguous social information that requires active interpretation. Their meaning is not fixed but constructed through dynamic interaction between the expresser, the observer, and the situational context in which the expression occurs (Aviezer et al., 2017). Because these factors jointly shape perception, the information conveyed by a facial configuration is often underspecified, leaving uncertainty about its precise emotional meaning (Jack et al., 2014). For instance, an angry or fearful face both indicate the presence of threat, but the degree of ambiguity differs regarding how imminent the threat is and whether it is directed towards the observer or someone else (Whalen, 1998). Similarly, a surprised face signals an unexpected event, leaving it uncertain whether the event is positive or negative (Neta and Kim, 2022).

Beyond stimulus properties, individual differences in IU likely shape how the same emotional faces are perceived and evaluated. IU exists on a continuum, capturing individual differences in sensitivity to uncertainty, as opposed to reactivity to explicit threat (Carleton et al., 2012). Cognitive models of anxiety propose that such differences can be understood as systematic information-processing biases, including interpretation, memory, and attentional biases (Beck and Clark, 1997; Mogg and Bradley, 1998). Among these, attentional bias, referring to an automatic tendency to orient towards threat-related cues, is particularly relevant to the present findings (Fergus et al., 2013; Fergus and Carleton, 2016). Individuals with high IU may show heightened vigilance toward the ambiguous features of emotional faces, perceiving their unpredictable social meaning as potentially threatening (FeldmanHall and Shenhav, 2019). Such hypervigilance, however, may extend beyond threat-specific processing to reflect a more general form of distractibility

characterized by increased attentional engagement with salient or task-irrelevant stimuli (Eysenck & Byrne, 1992; Fergus and Carleton, 2016). In this sense, hypervigilance in high-IU individuals may not necessarily indicate conscious threat perception but instead a sustained state of heightened environmental monitoring under uncertainty. Such a mechanism could lead to persistent amygdala engagement even when the emotional face stimuli are not overly threatening, reflecting a neural manifestation of generalized vigilance towards the unknown. From this perspective, a clearer understanding of whether amygdala habituation reflects modulation at the level of attentional allocation or subsequent stages of emotional interpretation may help to elucidate the neural processes that precede and support higher-order regulatory mechanisms, such as inhibitory learning and attentional monitoring (Morriss, 2025).

From a neurobiological perspective, the UAMA (Uncertainty–Anxiety–Motivation–Attention) framework suggests that hypervigilance in anxiety reflects a shift towards bottom-up, stimulus-driven processing, largely mediated by the amygdala (Grupe and Nitschke, 2013). The amygdala plays a central role in detecting salient or uncertain cues and triggering alerting responses that prepare the organism for potential threat (Rosen and Schulkin, 1998). Once the bottom-up influence becomes excessive, diminished top-down control can heighten attentional bias toward threat, maintaining vigilance that contributes to anxiety (Eysenck et al., 2007). While the amygdala serves as a central hub for detecting uncertainty and initiating vigilance, its function is best understood within this broader prefrontal-striatal network. The amygdala has rich, bidirectional connections with prefrontal and subcortical regions such as orbitofrontal cortex and ventral striatum, which are critically involved in the regulation of affective value, motivation, and expectancy (Ghashghaei and Barbas, 2002; Haber and Knutson, 2010). Through these pathways, heightened amygdala activity can bias expectancy and value appraisal, reinforcing vigilance towards uncertainty. This broader circuitry perspective provides a useful perspective for understanding how IU-related differences in vigilance may manifest in the brain as altered amygdala habituation over time.

Our finding that the moderating effect of IU remained significant after controlling for general trait anxiety underscores the unique contribution of IU to amygdala habituation. This result is consistent with previous studies showing that IU, beyond trait anxiety, uniquely predicts both behavioral and neural responses to uncertainty (Morriss et al., 2015; Fergus and Carleton, 2016; Morriss et al., 2021). Taken together, these findings suggest that neural sensitivity to uncertainty may underlie individual differences in IU, which in turn could serve as a transdiagnostic mechanism linking uncertainty processing to broader affective traits such as trait anxiety and related psychopathology.

Moreover, no significant IU-related effects were observed in the anterior insula. While the insula had been consistently associated with IU-related hyperactivity during uncertainty processing (Simmons et al., 2008; Gorka et al., 2016; Greifenberger et al., 2025), habituation to repeated emotional stimuli has been well characterized in the amygdala, drawing on animal models. That said, this null finding in anterior insula should be interpreted with several considerations in mind. The present control analyses employed a bilateral anterior insula mask encompassing a relatively broad region, which may have increased signal heterogeneity. Additionally, the present analysis focused on habituation to repeated face stimuli rather than overall levels of insular responsiveness; potential IU-related hyperactivity in the insula may require more fine-grained regional definitions and additional validation to be reliably characterized.

There are a number of limitations that could be addressed in future research. As the present study included only healthy participants, future research should examine whether similar IU-related neural patterns are evident in clinical populations with pathological anxiety. Given that IU has been identified as a transdiagnostic vulnerability factor underlying a wide range of anxiety and mood disorders, examining its neural dynamics in clinical groups may provide important insights into shared mechanisms of affective pathology (Einstein, 2014). Another caveat concerns the methodological aspect of the present experimental design. Because amygdala habituation occurs rapidly, future studies could employ methods with higher temporal resolution or comparative analytic time scale to better capture individual differences in neural dynamics. Previous work has emphasized the importance of modeling habituation beyond mean responses, highlighting the need for finer-grained analyses that capture trial-by-trial or short-term changes in neural activity (Lane et al., 2013; McDiarmid et al., 2017). While event-related designs are often used to assess such rapid habituation effects, block designs offer advantages in estimating stable activation patterns and longer-term habituation processes (Grill-Spector et al., 2006). Integrating these complementary approaches may clarify how IU shapes both transient and sustained aspects of amygdala adaptation to emotional uncertainty. In addition, future research could build on the present framework by examining dynamic fronto-amygdala connectivity. Such network-level analyses would require a more complex analytic framework and are therefore left for future investigation, while the present study focused on providing robust and tractable estimates of amygdala habituation. A further consideration concerns stimulus ordering. In the present study, emotional face stimuli were pseudo-randomized, which likely minimized order effects at the group level. However, because the order of emotional conditions differed across participants, the individually estimated slopes may have been influenced by block order variability. Although both analytic levels yielded convergent results, the group-level findings may provide a more reliable estimate of general patterns. Future studies should consider standardizing the sequence of emotional conditions or using emotion-specific task designs.

In conclusion, the present study examined how individual differences in intolerance of uncertainty shape the temporal dynamics of amygdala habituation to emotional faces. By focusing on uncertainty sensitivity rather than broader anxiety traits, this work highlights the neural relevance of how people adapt to uncertain emotional cues over time. While mean amygdala activation has been widely examined in prior research, investigating its temporal characteristics provides a complementary perspective that may deepen our understanding of how uncertainty shapes emotional brain responses and contributes to vulnerability for anxiety.

Acknowledgements

This work was supported by the National Research Foundation of Korea (NRF-2021S1A5A2A03070229).

Data and code availability statement

Codes for analyses are accessible at doi:10.5281/zenodo.17677507.

CRediT authorship contribution statement

Jihye Jeon: Writing – original draft, Visualization, Methodology, Formal analysis, Conceptualization. **Hakin Kim:** Data curation. **Juyoen Hur:** Supervision, Project administration. **M. Justin Kim:** Writing – review & editing, Supervision, Project administration, Funding acquisition, Conceptualization.

Declaration of competing interest

The authors declare that they have no known competing financial interests or personal relationships that could have appeared to influence the work reported in this paper.

Supplementary materials

Supplementary material associated with this article can be found, in

the online version, at doi:10.1016/j.neuroimage.2026.121691.

References

Aviezer, H., Ensenberg, N., Hassin, R.R., 2017. The inherently contextualized nature of facial emotion perception. Curr. Opin. Psychol. 17, 47–54. https://doi.org/10.1016/j.copsyc.2017.06.006.

Bates, D., Mächler, M., Bolker, B., Walker, S., 2015. Fitting Linear mixed-effects models using lme4. J. Stat. Softw. 67 (1), 1–48. https://doi.org/10.18637/jss.v067.i01.

Beck, A.T., Emery, G., Greenberg, R., 1985. Anxiety Disorders and Phobias: A Cognitive Perspective. Basic Books, New York.

Beck, A.T., Clark, D.A., 1997. An information processing model of anxiety: automatic and strategic processes. Behav. Res. Ther. 35 (1), 49–58. https://doi.org/10.1016/s0005-7967(96)00069-1.

Breiter, H.C., Etcoff, N.L., Whalen, P.J., Kennedy, W.A., Rauch, S.L., Buckner, R.L., Rosen, B.R., 1996. Response and habituation of the human amygdala during visual processing of facial expression. Neuron 17 (5), 875–887. https://doi.org/10.1016/s0896-6273(00)80219-6.

Bordi, F., LeDoux, J., 1992. Sensory tuning beyond the sensory system: an initial analysis of auditory response properties of neurons in the lateral amygdaloid nucleus and overlying areas of the striatum. J. Neurosci. 12 (7), 2493–2503. https://doi.org/10.1523/JNEUROSCI.12-07-02493.1992.

Buhr, K., Dugas, M.J., 2002. The intolerance of uncertainty scale: psychometric properties of the English version. Behav. Res. Ther. 40 (8), 931–945. https://doi.org/10.1016/s0005-7967(01)00092-4.

Carleton, R.N., 2016. Into the unknown: a review and synthesis of contemporary models involving uncertainty. J. Anxiety. Disord. 39, 30–43. https://doi.org/10.1016/j.janxdis.2016.02.007.

Carleton, R.N., Weeks, J.W., Howell, A.N., Asmundson, G.J.G., Antony, M.M., McCabe, R.E., 2012. Assessing the latent structure of the intolerance of uncertainty construct: an initial taxometric analysis. J. Anxiety. Disord. 26, 150–157. https://doi.org/10.1016/j.janxdis.2011.10.006.

Conley, M.I., Dellarco, D.V., Rubien-Thomas, E., Cohen, A.O., Cervera, A., Tottenham, N., Casey, B.J., 2018. The racially diverse affective expression (RADIATE) face stimulus set. Psychiatry Res. 270, 1059–1067. https://doi.org/10.1016/j.psychres.2018.04.066.

Cousineau, D., 2005. Confidence intervals in within-subject designs: a simpler solution to Loftus and Masson's method. Tutor. Quant. Methods Psychol. 1 (1), 42–45. https://doi.org/10.20982/tqmp.01.1.p042.

Cox, R.W., 1996. AFNI: software for analysis and visualization of functional magnetic resonance neuroimages. Comput. Biomed. Res. 29 (3), 162–173. https://doi.org/10.1006/cbmr.1996.0014.

Cox, R.W., Hyde, J.S., 1997. Software tools for analysis and visualization of fMRI data. NMR Biomed. 10 (4–5), 171–178. https://doi.org/10.1002/(sici)1099-1492(199706/08)10:4/5<171::aid-nbm453>3.0.co;2-l.

Davidson, R.J., 2002. Anxiety and affective style: Role of prefrontal cortex and amygdala. Biol. Psychiatry 51 (1), 68–80. https://doi.org/10.1016/S0006-3223(01)01328-2.

Davis, F.C., Neta, M., Kim, M.J., Moran, J.M., Whalen, P.J., 2016. Interpreting ambiguous social cues in unpredictable contexts. Soc. Cogn. Affect. Neurosci. 11 (5), 775–782. https://doi.org/10.1093/scan/nsw003.

Davis, M., Whalen, P.J., 2001. The amygdala: vigilance and emotion. Mol. Psychiatry 6, 13–34. https://doi.org/10.1038/sj.mp.4000812.

Dugas, M.J., Gosselin, P., Ladouceur, R., 2001. Intolerance of uncertainty and worry: investigating specificity in a nonclinical sample. Cogn. Ther. Res. 25, 551–558. https://doi.org/10.1023/A:1005553414688.

Dugas, M.J., Koerner, N., Freeston, M.H., 2025. State of the science: intolerance of uncertainty. Behav. Ther. https://doi.org/10.1016/j.beth.2025.08.009.

Dunsmoor, J.E., Campese, V.D., Ceceli, A.O., LeDoux, J.E., Phelps, E.A., 2015. Novelty-facilitated extinction: providing a novel outcome in place of an expected threat diminishes recovery of defensive responses. Biol. Psychiatry 78 (3), 203–209. https://doi.org/10.1016/j.biopsych.2014.12.008.

Einstein, D.A., 2014. Extension of the transdiagnostic model to focus on intolerance of uncertainty: a review of the literature and implications for treatment. Clin. Psychol. Sci. Pract. 21 (3), 280–300. https://doi.org/10.1111/cpsp.12077.

Esteban, O., Markiewicz, C.J., Blair, R.W., et al., 2019. fMRIPrep: a robust preprocessing pipeline for functional MRI. Nat. Methods 16 (1), 111–116. https://doi.org/10.1038/s41592-018-0235-4.

Eysenck, M.W., Byrne, A., 1992. Anxiety and susceptibility to distraction. Personal Individ. Differ. 13 (7), 793–798. https://doi.org/10.1016/0191-8869(92)90052-Q.

Eysenck, M.W., Derakshan, N., Santos, R., Calvo, M.G., 2007. Anxiety and cognitive performance: attentional control theory. Emotion. 7 (2), 336–353. https://doi.org/10.1037/1528-3542.7.2.336.

Fischer, H., Wright, C.I., Whalen, P.J., McInerney, S.C., Shin, L.M., Rauch, S.L., 2003. Brain habituation during repeated exposure to fearful and neutral faces: A functional MRI study. Brain Res. Bull. 59 (5), 387–392. https://doi.org/10.1016/S0361-9230(02)00938-1.

Freeston, M.H., Rhéaume, J., Letarte, H., Dugas, M.J., Ladouceur, R., 1994. Why do people worry? Personal Individ. Differ. 17 (6), 791–802. https://doi.org/10.1016/0191-8869(94)90048-5.

FeldmanHall, O., Shenhav, A., 2019. Resolving uncertainty in a social world. Nat. Hum. Behav. 3 (5), 426–435. https://doi.org/10.1038/s41562-019-0590-x.

Fergus, T.A., Bardeen, J.R., Wu, K.D., 2013. Intolerance of uncertainty and uncertainty-related attentional biases: evidence of facilitated engagement or disengagement difficulty? Cogn. Ther. Res. 37 (4), 735–741. https://doi.org/10.1007/s10608-012-9509-9.

Fergus, T.A., Carleton, R.N., 2016. Intolerance of uncertainty and attentional networks: unique associations with alerting. J. Anxiety. Disord. 41, 59–64. https://doi.org/10.1016/j.janxdis.2016.03.010.

Gee, D.G., McEwen, S.C., Forsyth, J.K., Haut, K.M., Bearden, C.E., Addington, J., Cannon, T.D., 2015. Reliability of an fMRI paradigm for emotional processing in a multisite longitudinal study. Hum. Brain Mapp. 36 (7), 2558–2579. https://doi.org/10.1002/hbm.22791.

Geissberger, N., Tik, M., Sladky, R., Woletz, M., Schuler, A.L., Willinger, D., Windischberger, C., 2020. Reproducibility of amygdala activation in facial emotion processing at 7T. NeuroImage, 116585. https://doi.org/10.1016/j.neuroimage.2020.116585.

Ghashghaei, H.T., Barbas, H., 2002. Pathways for emotion: interactions of prefrontal and anterior temporal pathways in the amygdala of the rhesus monkey. Neuroscience 115 (2002), 1261–1279. https://doi.org/10.1016/s0306-4522(02)00446-3.

Gorka, S.M., Nelson, B.D., Phan, K.L., Shankman, S.A., 2016. Intolerance of uncertainty and insula activation during uncertain reward. Cogn. Affect. Behav. Neurosci. 16 (5), 929–939. https://doi.org/10.3758/s13415-016-0443-2.

Greifenberger, A., Hill, G., Toumeh, E., Lokuge, S., Fotinos, K., Epstein, I., Katzman, M. A., 2025. Neurobiology of intolerance of uncertainty: a systematic review. J. Psychiatry Psychiatr. Disord. 9, 140–154. https://www.doi.org/10.26502/jppd.2572-519X0244.

Grill-Spector, K., Henson, R., Martin, A., 2006. Repetition and the brain: neural models of stimulus-specific effects. Trends. Cogn. Sci. 10 (1), 14–23. https://doi.org/10.1016/j.tics.2005.11.006.

Grupe, D.W., Nitschke, J.B., 2013. Uncertainty and anticipation in anxiety: an integrated neurobiological and psychological perspective. Nat. Rev. Neurosci. 14 (7), 488–501. https://doi.org/10.1038/nrn3524.

Haber, S.N., Knutson, B., 2010. The reward circuit: linking primate anatomy and human imaging. Neuropsychopharmacology 35, 4–26. https://doi.org/10.1038/npp.2009.129.

Hariri, A.R., Tessitore, A., Mattay, V.S., Fera, F., Weinberger, D.R., 2002. The amygdala response to emotional stimuli: a comparison of faces and scenes. Neuroimage 17 (1), 317–323. https://doi.org/10.1006/nimg.2002.1179.

Herry, C., Bach, D.R., Esposito, F., Di Salle, F., Perrig, W.J., Scheffler, K., Lüthi, A., Seifritz, E., 2007. Processing of temporal unpredictability in human and animal amygdala. J. Neurosci. 27 (22), 5958–5966. https://doi.org/10.1523/JNEUROSCI.5218-06.2007.

Jack, R.E., Garrod, O.G.B., Schyns, P.G., 2014. Dynamic facial expressions of emotion transmit an evolving hierarchy of signals over time. Curr. Biol. 24 (2), 187–192. https://doi.org/10.1016/j.cub.2013.11.064.

Kim, M.J., Knodt, A.R., Hariri, A.R., 2022. Meta-analytic activation maps can help identify affective processes captured by contrast-based task fMRI: The case of threat-related facial expressions. Soc. Cogn. Affect. Neurosci. 17 (9), 777–787. https://doi.org/10.1093/scan/nsac010.

Kim, M.J., Mattek, A.M., Bennett, R.H., Solomon, K.M., Shin, J., Whalen, P.J., 2017. Human amygdala tracks a feature-based valence signal embedded within the facial expression of surprise. J. Neurosci. 37 (39), 9510–9518. https://doi.org/10.1523/JNEUROSCI.1375-17.2017.

Kim, H., Somerville, L.H., Johnstone, T., Polis, S., Alexander, A.L., Shin, L.M., Whalen, P. J., 2004. Contextual modulation of amygdala responsivity to surprised faces. J. Neurosci. 16 (10), 1730–1745. https://doi.org/10.1162/0898929042947865.

Kim, Y.J., van Rooij, S.J.H., Ely, T.D., Fani, N., Ressler, K.J., Jovanovic, T., Stevens, J.S., 2019. Association between posttraumatic stress disorder severity and amygdala habituation to fearful stimuli. Depress. Anxiety. 36 (7), 647–658. https://doi.org/10.1002/da.22928.

Kleinhans, N.M., Johnson, L.C., Richards, T., Mahurin, R., Greenson, J., Dawson, G., Aylward, E., 2009. Reduced neural habituation in the amygdala and social impairments in autism spectrum disorders. Am. J. Psychiatry 166 (4), 467–475. https://doi.org/10.1176/appi.ajp.2008.07101681.

Lane, S.T., Franklin, J.C., Curran, P.J., 2013. Clarifying the nature of startle habituation using latent curve modeling. Int. J. Psychophysiol. 88 (1), 55–63. https://doi.org/10.1016/j.ijpsycho.2013.01.010.

Lenth, R.V., 2023. Emmeans: Estimated Marginal Means, Aka Least-Squares Means (R package version 1.8.9). https://CRAN.R-project.org/package=emmeans.

McDiarmid, T.A., Bernardos, A.C., Rankin, C.H., 2017. Habituation is altered in neuropsychiatric disorders—a comprehensive review with recommendations for experimental design and analysis. Neurosci. Biobehav. Rev. 80, 286–305. https://doi.org/10.1016/j.neubiorev.2017.05.028.

Mende-Siedlecki, P., Verosky, S.C., Turk-Browne, N.B., Todorov, A., 2013. Robust selectivity for faces in the human amygdala in the absence of expressions. J. Cogn. Neurosci. 25 (12), 2086–2106. https://doi.org/10.1162/jocn_a_00469.

Mogg, K., Bradley, B.P., 1998. A cognitive-motivational analysis of anxiety. Behav. Res. Ther. 36 (9), 809–848. https://doi.org/10.1016/s0005-7967(98)00063-1.

Morey, R.D., 2008. Confidence intervals from normalized data: A correction to Cousineau (2005). Tutor. Quant. Methods Psychol. 4 (2), 61–64. https://doi.org/10.20982/tqmp.04.2.p061.

Morriss, J., Abend, R., Zika, O., Bradford, D.E., Mertens, G., 2023. Neural and psychophysiological markers of intolerance of uncertainty. Int. J. Psychophysiol. 184, 94–99. https://doi.org/10.1016/j.ijpsycho.2023.01.003.

Morriss, J., Christakou, A., van Reekum, C.M., 2015. Intolerance of uncertainty predicts fear extinction in amygdala–ventromedial prefrontal cortical circuitry. Biol. Mood. Anxiety. Disord. 5, 4. https://doi.org/10.1186/s13587-015-0019-8.

Morriss, J., Christakou, A., van Reekum, C.M., 2016b. Nothing is safe: Intolerance of uncertainty is associated with compromised fear extinction learning. Biol. Psychol. 121 (Pt B), 187–193. https://doi.org/10.1016/j.biopsycho.2016.05.001.

Morriss, J., Macdonald, B., van Reekum, C.M., 2016a. What is going on around here? Intolerance of uncertainty predicts threat generalization. PLoS. One 11 (5), e0154494. https://doi.org/10.1371/journal.pone.0154494.

Morriss, J., 2025. Psychological mechanisms underpinning change in intolerance of uncertainty across anxiety-related disorders: New insights for translational research. Neurosci. Biobehav. Rev. 173, 106138. https://doi.org/10.1016/j.neubiorev.2025.106138.

Morriss, J., Wake, S., Elizabeth, C., van Reekum, C.M., 2021. I doubt it is safe: A meta-analysis of self-reported intolerance of uncertainty and threat extinction training. Biol. Psychiatry Glob. Open. Sci. 1 (3), 171–179. https://doi.org/10.1016/j.bpsgos.2021.05.011.

Neta, M., Kim, M.J., 2022. Surprise as an Emotion: A Response to Ortony. Perspect. Psychol. Sci. 18 (4), 854–862. https://doi.org/10.1177/17456916221132789.

Phillips, M.L., Medford, N., Young, A.W., Williams, L., Williams, S.C., Bullmore, E.T., Gray, J.A., Brammer, M.J., 2001. Time courses of left and right amygdalar responses to fearful facial expressions. Hum. Brain Mapp. 12, 193–202. https://doi.org/10.1002/1097-0193(200104)12:4<193::aid-hbm1015>3.0.co;2-a.

Plichta, M.M., Grimm, O., Morgen, K., Mier, D., Sauer, C., Haddad, L., Tost, H., Esslinger, C., Kirsch, P., Schwarz, A.J., Meyer-Lindenberg, A., 2014. Amygdala habituation: a reliable fMRI phenotype. Neuroimage 103, 383–390. https://doi.org/10.1016/j.neuroimage.2014.09.059.

Rankin, C.H., Abrams, T., Barry, R.J., Bhatnagar, S., Clayton, D.F., Colombo, J., Thompson, R.F., 2009. Habituation revisited: An updated and revised description of the behavioral characteristics of habituation. Neurobiol. Learn. Mem. 92, 135–138. https://doi.org/10.1016/j.nlm.2008.09.012.

Rosen, J.B., Donley, M.P., 2006. Animal studies of amygdala function in fear and uncertainty: Relevance to human research. Biol. Psychol. 73 (1), 49–60. https://doi.org/10.1016/j.biopsycho.2006.01.007.

Rosen, J.B., Schulkin, J., 1998. From normal fear to pathological anxiety. Psychol. Rev. 105 (2), 325–350. https://doi.org/10.1037/0033-295X.105.2.325.

Silverman, M.H., Wilson, S., Ramsay, I.S., Hunt, R.H., Thomas, K.M., Krueger, R.F., Iacono, W.G., 2019. Trait neuroticism and emotion neurocircuitry: Functional magnetic resonance imaging evidence for a failure in emotion regulation. Dev. Psychopathol. 31 (3), 1085–1099. https://doi.org/10.1017/S0954579419000610.

Simmons, A., Matthews, S.C., Paulus, M.P., Stein, M.B., 2008. Intolerance of uncertainty correlates with insula activation during affective ambiguity. Neurosci. Lett. 430 (2), 92–97. https://doi.org/10.1016/j.neulet.2007.10.030.

Somerville, L.H., Kim, H., Johnstone, T., Alexander, A.L., Whalen, P.J., 2004. Human amygdala responses during presentation of happy and neutral faces: correlations with state anxiety. Biol. Psychiatry 55 (9), 897–903. https://doi.org/10.1016/j.biopsych.2004.01.007.

Schienle, A., Köchel, A., Ebner, F., Reishofer, G., Schäfer, A., 2010. Neural correlates of intolerance of uncertainty. Neurosci. Lett. 479 (3), 272–276. https://doi.org/10.1016/j.neulet.2010.05.078.

Schuyler, B.S., Kral, T.R., Jacquart, J., Burghy, C.A., Weng, H.Y., Perlman, D.M., Bachhuber, D.R., Rosenkranz, M.A., Maccoon, D.G., van Reekum, C.M., Lutz, A., Davidson, R.J., 2014. Temporal dynamics of emotional responding: amygdala recovery predicts emotional traits. Soc. Cogn. Affect. Neurosci. 9 (2), 176–181. https://doi.org/10.1093/scan/nss131.

Shin, L.M., Wright, C.I., Cannistraro, P.A., Wedig, M.M., McMullin, K., Martis, B., Macklin, M.L., Lasko, N.B., Cavanagh, S.R., Krangel, T.S., Orr, S.P., Pitman, R.K., Whalen, P.J., Rauch, S.L., 2005. A functional magnetic resonance imaging study of amygdala and medial prefrontal cortex responses to overtly presented fearful faces in posttraumatic stress disorder. Arch. Gen. Psychiatry 62 (3), 273–281. https://doi.org/10.1001/archpsyc.62.3.273.

Spielberger, C. D. (1983). *State-Trait Anxiety Inventory for Adults*. APA PsycTests. https://doi.org/10.1037/t06496-000.

Stevens, J.S., Hamann, S., 2012. Sex differences in brain activation to emotional stimuli: a meta-analysis of neuroimaging studies. Neuropsychologia 50 (7), 1578–1593. https://doi.org/10.1016/j.neuropsychologia.2012.03.011.

Swartz, J.R., Wiggins, J.L., Carrasco, M., Lord, C., Monk, C.S., 2013. Amygdala habituation and prefrontal functional connectivity in youth with autism spectrum disorders. J. Am. Acad. Child Adolesc. Psychiatry 52 (1), 84–93. https://doi.org/10.1016/j.jaac.2012.10.012.

Tanovic, E., Gee, D.G., Joormann, J., 2018. Intolerance of uncertainty: Neural and psychophysiological correlates of the perception of uncertainty as threatening. Clin. Psychol. Rev. 60, 87–99. https://doi.org/10.1016/j.cpr.2018.01.001.

Thompson, R.F., Spencer, W.A., 1966. Habituation: a model phenomenon for the study of neuronal substrates of behavior. Psychol. Rev. 73 (1), 16–43. https://doi.org/10.1037/h0022681.

Williams, L.E., Blackford, J.U., Luksik, A., Gauthier, I., Heckers, S., 2013. Reduced habituation in patients with schizophrenia. Schizophr. Res. 151 (1-3), 124–132. https://doi.org/10.1016/j.schres.2013.10.017.

Whalen, P.J., 1998. Fear, vigilance, and ambiguity: Initial neuroimaging studies of the human amygdala. Curr. Dir. Psychol. Sci. 7 (6), 177–188. https://doi.org/10.1111/1467-8721.ep10836912.

Whalen, P.J., Shin, L.M., McInerney, S.C., Fischer, H., Wright, C.I., Rauch, S.L., 2001. A functional MRI study of human amygdala responses to facial expressions of fear versus anger. Emotion 1 (1), 70–83. https://doi.org/10.1037/1528-3542.1.1.70.